https://doi.org/10.5194/wes-2023-80
Preprint. Discussion started: 8 August 2023

eawe european academy of wind energy
Open Access WIND ENERGY SCIENCE DISCUSSIONS

Uncertainty quantification of structural blade parameters for the aeroelastic damping of wind turbines: a code-to-code comparison

Hendrik Verdonck[1], Oliver Hach[1], Jelmer D. Polman[2], Otto Braun[2], Claudio Balzani[2], Sarah Müller[3], and Johannes Rieke[3]

[1]German Aerospace Center (DLR), Institute of Aeroelasticity, Germany
[2]Leibniz University Hannover, Institute for Wind Energy Systems, Germany
[3]Nordex Energy SE & Co. KG, Germany

Correspondence: Hendrik Verdonck (hendrik.verdonck@dlr.de)

Abstract. Uncertainty quantification (UQ) is a well-established category of methods to estimate the effect of parameter variations on a quantity of interest, based on a solid mathematical fundament. In the wind energy field most UQ studies were focused on the sensitivity of turbine loads. This article presents a framework, wrapped around a modern Python UQ library, to analyze the impact of uncertain turbine properties on aeroelastic stability. The UQ methodology applies a polynomial chaos expansion surrogate model to increase the numerical efficiency. A comparison is made between different wind turbine simulation tools on the engineering model level (alaska/Wind, Bladed, HAWC2/HAWCStab2 and Simpack). Two case studies are used to demonstrate the effectiveness of the method to analyze the sensitivity of the aeroelastic damping of an unstable turbine mode to variations of structural blade cross section parameters. The code-to-code comparison shows a good agreement between the simulation tools for the reference model, but also significant differences in the sensitivities.

1 Introduction

The size of wind turbines has been rapidly increasing over the last decades. As a consequence, current wind turbine blades are more slender and flexible than ever before (Veers et al., 2019). This increases the complexity of turbine vibrations and potentially the probability of aeroelastic instabilities, which raises the questions which kind of instabilities are more likely to appear, how state-of-the-art simulation tools compare in their capability to predict this kind of behavior and how these instabilities can be prevented. Volk et al. (2020) and Kallesøe and Kragh (2016) showed in an experimental validation on a 7 MW, 154 m diameter turbine that instabilities dominated by 1st and 2nd edgewise modes arise when a modern wind turbine is operated in overspeed.

The required multi-disciplinary models to numerically represent these phenomena are complex and have a significant computational cost. Typical models used in the industry and research employ a multi-body description with beam models for the flexible bodies and Blade Element Momentum (BEM) models, with semi-empirical unsteady extensions, for the aerodynamics. The linear stability behavior is commonly investigated by a linearization of the governing equations around a steady state equilibrium of the non-linear system. These models and solution routines depend on numerous parameters, which complicates

https://doi.org/10.5194/wes-2023-80
Preprint. Discussion started: 8 August 2023

eawe european academy of wind energy
Open Access WIND ENERGY SCIENCE DISCUSSIONS

the identification of the key factors that influence the observed stability behavior. Global uncertainty quantification (UQ) can help identify these crucial factors.

Uncertainty quantification has been a relevant topic in almost all scientific fields. In engineering, it is commonly used to understand physical systems, to improve the design robustness, as preprocessing step towards model updating and model calibration or as a component of optimization procedures (Sankararaman, 2012). A comprehensive overview of methods for global sensitivity analysis is given by Iooss and Lemaître (2015). The focus in this paper is on variance-based methods which give a detailed, non-linear description of the uncertainty in a system, including interactions between parameters. A promising approach to allow detailed global sensitivity analysis on computationally expensive simulations, is the introduction of a surrogate model to approximate the full system. Polynomial Chaos Expansion (PCE) models are becoming increasingly popular for this purpose (e.g., Sudret, 2008; Le Gratiet et al., 2017; Abbiati et al., 2021; Eldred and Burkardt, 2009). PCE models span the full uncertainty domain with a set of orthogonal polynomials. The coefficients of the polynomials are determined by a regression based on samples of the true model. A literature overview on UQ studies in the wind energy field is given by van den Bos and Sanderse (2017). Most research efforts have the wind turbine design loads as quantity of interest (e.g., Roberson et al., 2019; Ziegler and Muskulus, 2016; Gonzaga et al., 2022). Multiple authors successfully applied a surrogate model based UQ approach to handle the significant computational cost of the load computations (e.g., Bortolotti et al., 2019; Kumar et al., 2020; Caboni et al., 2020; Hübler et al., 2017, 2019). Comparatively few studies have been performed on uncertainties in wind turbine stability analysis. Resor and Paquette (2011), Lobitz (2005), and Pourazarm et al. (2015b, a) evaluated the impact of uncertainties in the structural and aerodynamic modeling on the flutter speed of an isolated blade by a manual and independent variation of the uncertainty sources. Li and Caracoglia (2019) compared different setups of a polynomial based surrogate model for the UQ of two interacting uncertain parameters on the flutter speed of an isolated blade. Literature on the uncertainty quantification of full wind turbine stability phenomena is not known to the authors.

To fill this gap, the present article describes a comprehensive methodology for the uncertainty quantification of wind turbine stability analysis. The effect of uncertain beam properties in the elastic blade model on an edgewise whirl wind turbine instability are analyzed. Multiple aeroelastic simulation tools are used in a code-to-code comparison to investigate the influence of the simulation tools on the uncertainty prediction.

In the default configuration, the IWT-7.5-164 reference wind turbine (Popko et al., 2018) as used in this project shows no aeroelastic instability in the normal operational range. An instability, however, is needed for quantifying the uncertainties. Thus, a change in the blade stiffness was applied, such that an edgewise whirl instability formed, similar to those experimentally shown by Volk et al. (2020). This reference condition is simulated with the state-of-the-art simulation tools alaska/Wind, Bladed, HAWC2/HAWCStab2, and Simpack. An OpenFAST model of the reference turbine was established and used for the verification of the other models. However, a stability assessment has not been made with this model, because the enforcement of the aeroelastic instability was not successful in this case. The critical reference condition and a detailed comparison of the results for the presented tools are described in Sect. 2. On this basis, uncertainty quantification is done with respect to the influence of beam properties on the instability. Two academic case studies are performed to show the capabilities of this

https://doi.org/10.5194/wes-2023-80
Preprint. Discussion started: 8 August 2023

eawe european academy of wind energy
Open Access WIND ENERGY SCIENCE DISCUSSIONS

methodology and to show the comparability and differences in the results between the different simulation tools. This is shown in Sect. 3.

2 Critical reference condition

This section will first describe the wind turbine reference model and the required model modifications to create an interesting instability phenomenon. The wind turbine simulation tools are introduced and the main verification results with this new model are presented. Finally, the critical unstable reference condition is analyzed in detail.

2.1 Reference model

The IWT-7.5-164 open-source reference turbine is used as baseline configuration (Popko et al., 2018). This turbine was designed according to the environmental conditions defined for wind turbine class IA (IEC, 2005). A detailed code-to-code comparison of this turbine with a focus on the stability behavior with the proposed tools has been presented in Hach et al. (2020). The baseline model has been modified in a couple of aspects. The current work focuses on instabilities. Therefore, all asymmetries are excluded from the model to eliminate periodic excitation and resonance effects. This means no gravitational loads, no rotor tilt or yaw, a uniform wind profile, and no tower influence on the wind field. Note that the tower deflection causes a tilting effect on the rotor plane and the corresponding asymmetry. This effect can not be eliminated, but causes only a negligible periodic excitation. Further noteworthy modifications are the fixed operating conditions, which eliminates the need for an active control system, and the rigid clamping at the root of the tower.

Different techniques can be used to introduce an instability for this baseline reference turbine. As presented by Pirrung et al. (2014), the turbine can be operated in a runaway setting. In this kind of simulation, the wind speed increases gradually and without counteracting generator torque the rotor will accelerate until an instability arises. This procedure has the disadvantage that the operating condition at the instability varies between tools, as shown for the IWT turbine in Hach et al. (2020). This introduces an additional uncertainty and might complicate the comparison between said tools. Additionally, the runaway critical operating condition might be far above nominal rotor speeds, reducing the comparability with realistic operational conditions. Instead, the physical properties of the turbine are manipulated in order to enforce an instability under nominal operating conditions. A priori, the sensitivity of the turbine stability on the model parameters was unknown. The model manipulation was therefore a trial-and-error process based on engineering knowledge. Only the flapwise, edgewise and torsional stiffness of the blades were modified with a uniform scaling factor along the blade, to keep the parameter space limited. The stiffness reductions were done on the 6x6 stiffness matrices, which were computed with BECAS (Blasques et al., 2016), and served as reference for all other tools. The resulting aeroelastic behavior for different sets of scaling factors was analyzed iteratively in HAWCStab2. A stiffness reduction of 70% in flapwise direction, 30% in edgewise direction, and 70% in torsional direction was required to accomplish the desired instability behavior.

https://doi.org/10.5194/wes-2023-80
Preprint. Discussion started: 8 August 2023

eawe european academy of wind energy
Open Access WIND ENERGY SCIENCE DISCUSSIONS

2.2 Wind turbine simulation tools

In this research, a comparison is made between multiple state-of-the-art aeroelastic simulation tools. All tools are based on the same category of low-fidelity engineering models. The main model properties are summarized in table 1. Preliminary comparisons have indicated that it is crucial to capture both the geometric coupling effects and nonlinear deformations of the blades, in addition to accounting for unsteady aerodynamic effects. Some differences exist in the corresponding theories underlying the implementations in the different tools. The structural blade models in alaska/Wind, HAWC2, and OpenFAST use the reference 6x6 mass and stiffness matrices directly for an exact model of the geometric coupling effects. Bladed and Simpack use beam properties derived from the 6x6 matrices which include coupling effects due to offsets between the shear and elastic centers. Geometrically non-linear effects are incorporated through a multi-body segmentation in Bladed, HAWC2, and Simpack, while alaska/Wind and OpenFAST use a direct internal non-linear finite element analysis. All tools use a Beddoes-Leishman-like dynamic stall model. Alaska/Wind, Bladed, and HAWC2 additionally include a dynamic wake model, which was not available for the OpenFAST and Simpack models.

Two analysis methods are used for the stability assessment, depending on the available functionalities of the tools. Bladed and HAWC2/HAWCStab2 offer the functionality to linearize their models around a non-linear equilibrium point, which is the standard approach for stability assessment. As alternative approach, non-linear time domain simulations are made in all tools followed by a postprocessing methodology on the time series which will be discussed in Sect. 2.4.

Table 1. Overview of the features of the used simulation tools

Model	**alaska/Wind**	**Bladed**	**HAWC2**	**OpenFAST**	**Simpack-AeroDyn**
Version	9.6	4.9	12.8	2.2.0	2019x.2 - ADv13
Tower structure	Modal[1], MD	Modal[1], MD	Modal[1], RD	Modal[1], MD	Modal[2], MD
Blade structure	FE[2], RD	Modal[3], MD	Modal[2,3], RD	FE[1,2], RD	Modal[3], MD
Rotor aerodynamics	BEM, BL, DF	BEM, BL, ODW	BEM, BL, DI	BEM, BL	BEM, BL
Linearization	/	Bladed (lin.)	HAWCStab2	/	/

FE: *Finite Elements* MD: *Modal Damping* RD: *Rayleigh Damping*

[1] *single body, internal Finite Element Analysis (FEA)*

[2] *internal model based on 6×6 mass and stiffness matrices*

[3] *multi-body, internal FEA*

BEM: *Blade Element Momentum theory* BL: *Beddoes-Leishman dynamic stall model*

DF: *Dynamic Flex wake model* ODW: *Øye Dynamic Wake model* DI: *Dynamic Inflow model*

https://doi.org/10.5194/wes-2023-80
Preprint. Discussion started: 8 August 2023

eawe european academy of wind energy
Open Access WIND ENERGY SCIENCE DISCUSSIONS

2.3 Model verification

The simulation tools used in this work were previously compared for the same reference turbine but without the stiffness reductions by Hach et al. (2020). A similar strategy with test cases of increasing complexity was also applied for this new reduced stiffness reference model. The most notable results are discussed here.

The isolated, clamped blade eigenfrequencies are shown in figure 1. All tools are in excellent agreement. The relative difference between the tools is less than 0.5% for the first five modes. The deviations increase for higher frequency modes, but remain below, or close to, 1%. The Simpack eigenfrequencies show the largest deviation, especially for modes with a high torsional content.

As second comparison, a steady quintuple gravitational load is imposed on the clamped blades. The blades are positioned both with the suction side downwards, such that gravitational loading is in flapwise direction and with the leading edge downwards, such that the gravitational loading is in edgewise direction. The gravitational loading multiple is representative for nominal operational loads. The results for the flapwise loading are shown in the left column of figure 2 and for the edgewise loading in the right column. The translational deflections in the direction of the loading are in excellent agreement. Small deviations arise for the deflections in the direction perpendicular to the loading, especially for the flapwise deflection under edgewise loading. The main point of difference is the representation of the torsional component. Significant differences exist between all tools with discrepancies up to 0.5°. The unphysical oscillations towards the tip in the OpenFAST result were also observed in Hach et al. (2020) and are likely due to a faulty blade curvature and twist calculation with the internal cubic spline fit in BeamDyn (NREL, 2019).

The final verification test shows the static aeroelastic equilibrium for a rotor system with rigid tower in a uniform, steady wind field with a velocity of 10 m/s. The rotor blades are in this test the only only flexible component of the turbine. The steady state aerodynamic loads are shown in the left column of figure 3, the corresponding steady state deflections are shown on the right-hand side. Due to the increased complexity, the agreement between the tools deteriorated in comparison with the static deformation case above. Nevertheless, the overall agreement is reasonable. Alaska/Wind shows the largest discrepancy with respect to the other tools, with lower loads in all directions and therefore also consistently lower deformations. The OpenFAST result shows here as well the unphysical oscillation in the torsional deformation near the tip of the blade.

2.4 Damping determination from time domain simulations

To allow a stability assessment based on the time domain simulations, the damping of the system has to be determined from the resulting time signals. Multiple approaches can be used to achieve this. Riziotis and Voutsinas (2006) used two different methods: the first method was based on the gradient of peaks in the amplitude spectrum of a moving FFT window, the second method was applied directly on the signal amplitude envelope by means of a Hilbert transform. Volk et al. (2020) used logarithmic decrement analysis on a signal after a bandpass filter was applied around a predefined frequency. Wanke et al. (2020) used an exponential fitting on the oscillatory signal after excitation on the three blades at the desired frequency and desired phase difference between the blades.

https://doi.org/10.5194/wes-2023-80
Preprint. Discussion started: 8 August 2023

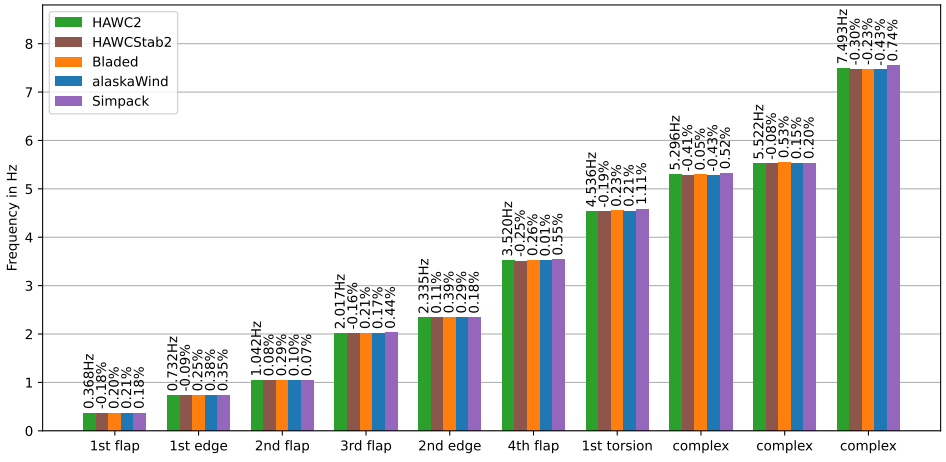

Figure 1. Comparison of isolated blade eigenfrequencies

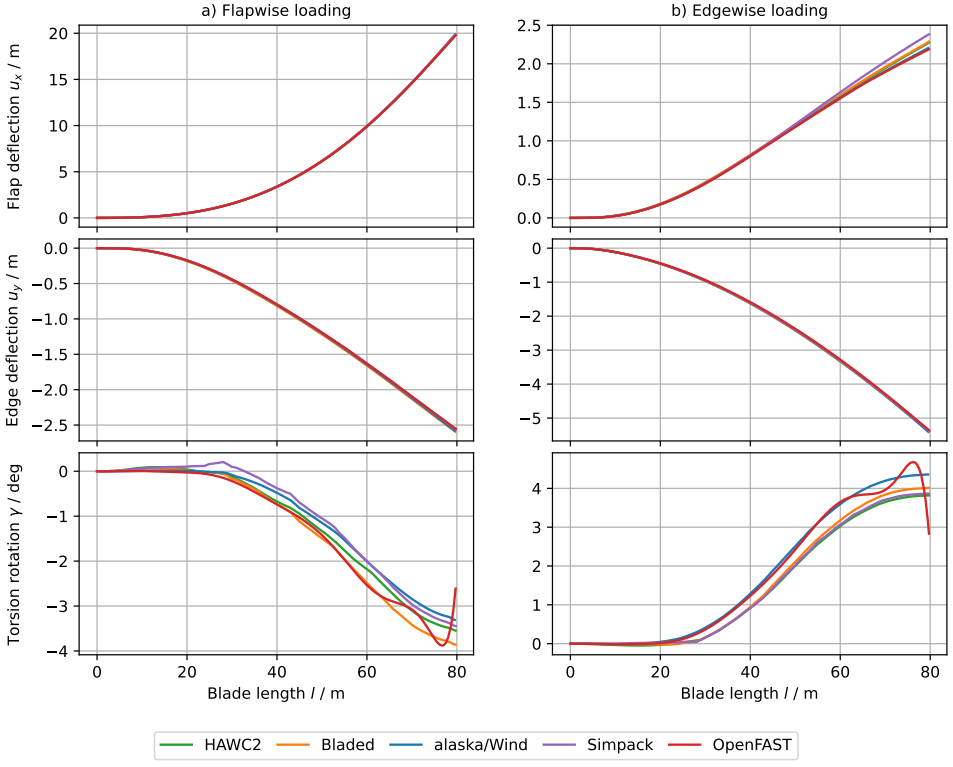

Figure 2. Comparison of isolated blade deflections under steady quintuple gravitational loads

https://doi.org/10.5194/wes-2023-80
Preprint. Discussion started: 8 August 2023

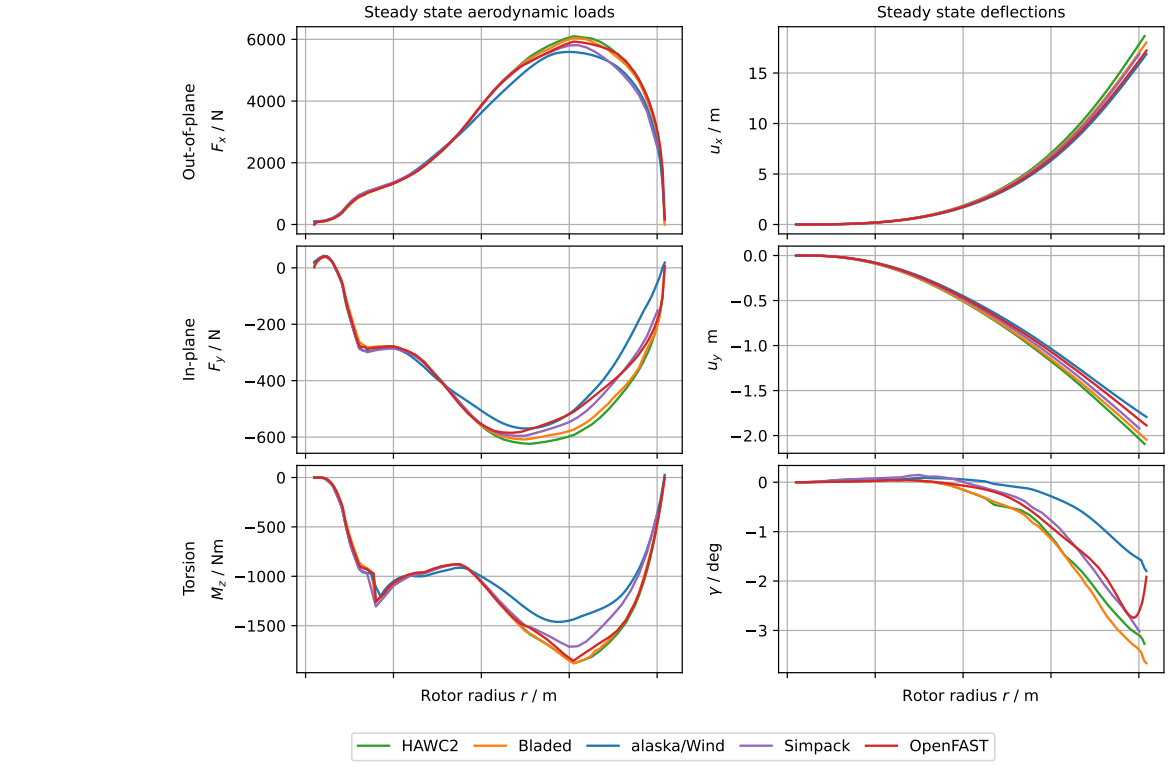

Figure 3. Comparison of the aeroelastic steady state loads and deflections of the full rotor

In this work, a different approach based on the Dynamic Mode Decomposition (DMD) method is used. The higher order DMD formulation by Le Clainche and Vega (2017) was applied, which is available in the open-source Python package pyDMD. For a detailed theoretical description of the method, please refer to Le Clainche and Vega (2017). This method describes the signal in a spatio-temporal manner, i.e., it can be used to decompose a signal in spatial modes with corresponding frequency and damping content. For linear aeroelastic systems, this would mean that the exact physical modes can be extracted. For non-linear systems, DMD can be understood as a best-fit linear operator on the non-linear signal. This method is fully data-driven, which is an important characteristic if the methodology has to be applied onto simulation tools with restricted access to the source code. The only required inputs are snapshots of the time signals. Note that these signals were transformed into the inertial reference system with a multiblade coordinate transformation (MBC) (Bir, 2008). The accuracy and robustness of DMD can depend strongly on the selection of these snapshots and the configuration parameters of the DMD method. The configurable parameters and their selected settings are shown in table 2. It is worth to mention that a fully automated post-processing has not been achieved. Some of the parameters in table 2 cannot be applied equally for all the results. A full list of the choices is beyond the scope of this article, but it is part of the data package published in <todo>.

For completeness, it is important to mention that a number of other methods to determine the damping from time signals were attempted without success. Computing the logarithmic decrement from subsequent oscillation peaks, exponential curve

https://doi.org/10.5194/wes-2023-80
Preprint. Discussion started: 8 August 2023

eawe european academy of wind energy
Open Access WIND ENERGY SCIENCE DISCUSSIONS

Table 2. DMD damping determination settings

Parameter	Selected setting
Variable selection	The algorithm works better with more signals. The selected degrees of freedom should be a good identifier for the interested modes. At least 18 torsion and in-plane deflection signals were used.
Snapshot window selection	A snapshot has to be selected from the time signals. This snapshot has to be placed at the beginning of the instability, where the DMD assumption of a linear system is most valid. The window length should be as long as possible, yet only as long as the system behaves quasi-linearly.
Signal downsampling	Downsampling of the signal to 8 Hz resulted in a more robust identification on the signals of some of the tools (alaska/Wind, HAWC2 and Simpack).
SVD rank	The SVD rank in the DMD algorithm determines how many modes will be identified. A smaller SVD rank of 20 modes resulted in the best identification in all tools.

fitting on the oscillation peaks and linear curve fitting on logarithmic data all share the assumption that the signal only has a single degree of freedom. Their accuracy is largely dependent on a smooth, linear signal and they did therefore not produce robust results for the multi-degree of freedom, non-linear results of the wind turbine simulation tools. Attempts with bandpass filtering the signal for a specific frequency range did not lead to robustness improvements.

2.5 Comparison between Campbell plots and time domain runs

The final stability analysis of the reference condition is shown as a Campbell diagram in Fig. 4. This reference condition was presented earlier in Verdonck et al. (2021), but will be discussed here in more detail. Figure 4a shows the HAWCStab2 and Bladed (lin.)[1] linearization results. Only 1st and 2nd edgewise whirling modes are visualized. These are the only modes of the system which become unstable. One can see an almost exact match in the frequency progression between the tools. The trend of the damping curves is also in agreement. The 1st edgewise backward whirling (BW) and forward whirling (FW) modes have a double dip trend with the most negative damping values around 10 and 13 m/s. The 2nd edgewise BW and FW modes show a steady decrease in damping until 12 m/s, followed by a consistent increase. The absolute damping values show some differences. The HAWCStab2 damping is lower for the 1st edgewise BW mode and the 2nd edgewise modes. The opposite is true for the 1st edgewise FW mode. The absolute differences for the 1st edgewise modes are significantly smaller than the differences for the 2nd edgewise modes.

Figures 4b-4e show the comparison with each of the time domain tools. Time domain simulations were executed at each of the 8 wind speeds (8, 9, ..., 15 m/s). As described in Sect. 2.4, the MBC transformed time signals were postprocessed with DMD to obtain the modal content in the signal. These results are shown by the colorful hexagonal markers in both the

[1] **Remark:** It has to be mentioned that the damping of a Bladed linearization with multiple operating points can differ slightly from the damping of a linearization performed for a single operating point (as will be done for the UQ studies in Sect. 3). This numerical artefact only occurs if unsteady aerodynamic models are used and is likely caused by an incorrect re-initialization between subsequent operating points. The simulations in this study were made with Bladed 4.9. This issue will be solved in a later release.

https://doi.org/10.5194/wes-2023-80
Preprint. Discussion started: 8 August 2023

frequency and damping plots. The size of these markers indicates their participation in the signal. This is particularly useful to identify modes which have a significant participation in unstable signals. The color scale of the markers indicates the frequency of the mode, to be able to link the DMD markers between the damping and frequency plot. The HAWCStab2 and Bladed (lin.) linearization results are repeated in each of these plots by the grey lines in the background. First, the overall results of the DMD postprocessing of the time domain tools in comparison to the linearizations will be discussed, followed by a discussion of the most noticeable deviations or details of the individual tools.

Overall, clear correlations between the DMD postprocessed time series and the linearizations can be found. The time domain simulations of almost all tools are unstable in the same wind speed range from 10 m/s up to 15 m/s. For most tools, the 1st and 2nd edgewise modes are identified accurately for the unstable time simulations. Moreover, a similar trend over the wind speeds appears. The 1st edgewise BW mode has the lowest damping at low and high wind speeds (9-10 m/s and 13-15 m/s), but a slightly higher and sometimes positive damping around rated wind speeds (11-12 m/s). On the other hand, the damping of the 2nd edgewise BW mode monotonously decreases up to 12 m/s and increases afterwards. This results in almost all tools in an instability mechanism dominated by the 1st edgewise BW mode at lower wind speeds (< 11 m/s), dominated by the 2nd edgewise modes at the middle wind speeds (11-12 m/s), and dominated again by the 1st edgewise mode at higher wind speeds (> 12 m/s). The DMD setup in this project is tuned to identify the unstable or marginally stable modes. The application of the same method to stable or highly damped time series was out of the scope. This makes that the applied methodology is not suitable for stable operating points (e.g. 8 m/s), where a poor agreement between the DMD processed time series and the linearizations can be found. In order to generate a full Campbell diagram, the DMD identification of all modes, regardless of their damping, could be subject for further studies.

A closer look at the DMD results of the individual tools shows following peculiarities. The HAWC2 time domain results agree on the whole well with the HAWCStab2 linearization. Two small differences are the overall slightly lower frequency of the 2nd edgewise BW mode and the higher damping of this same mode at 11 and 12 m/s. The Bladed time domain simulations are only unstable for the operating points between 10 m/s and 13 m/s. The identified 2nd edgewise BW mode matches both in frequency and damping excellently with the Bladed linearization. The 1st edgewise BW modal component is also identified, but its participation in the time signal and damping ratio is higher compared to the linearization results and the other time domain simulations. This explains why the time simulations with Bladed are stable at 14 m/s and 15 m/s, where the other tools experience 1st edgewise BW dominated instability mechanisms. In alaska/Wind, the 1st edgewise FW mode has a significantly lower damping compared to all other tools. At 10 m/s this even becomes the lowest damped mode. The frequency of the 2nd edgewise BW mode is also slightly below the linearization results. Besides this, the trend and magnitude of both the frequencies and damping of the 1st and 2nd edgewise BW modes agrees well with the linearizations. The Simpack results show some significant differences with respect to the linearizations and the other tools. The 2nd edgewise modes have a significantly lower frequency. Furthermore, although the trend correlates well with the linearizations, the magnitude of the damping of the 1st and 2nd edgewise modes is significantly lower.

https://doi.org/10.5194/wes-2023-80
Preprint. Discussion started: 8 August 2023

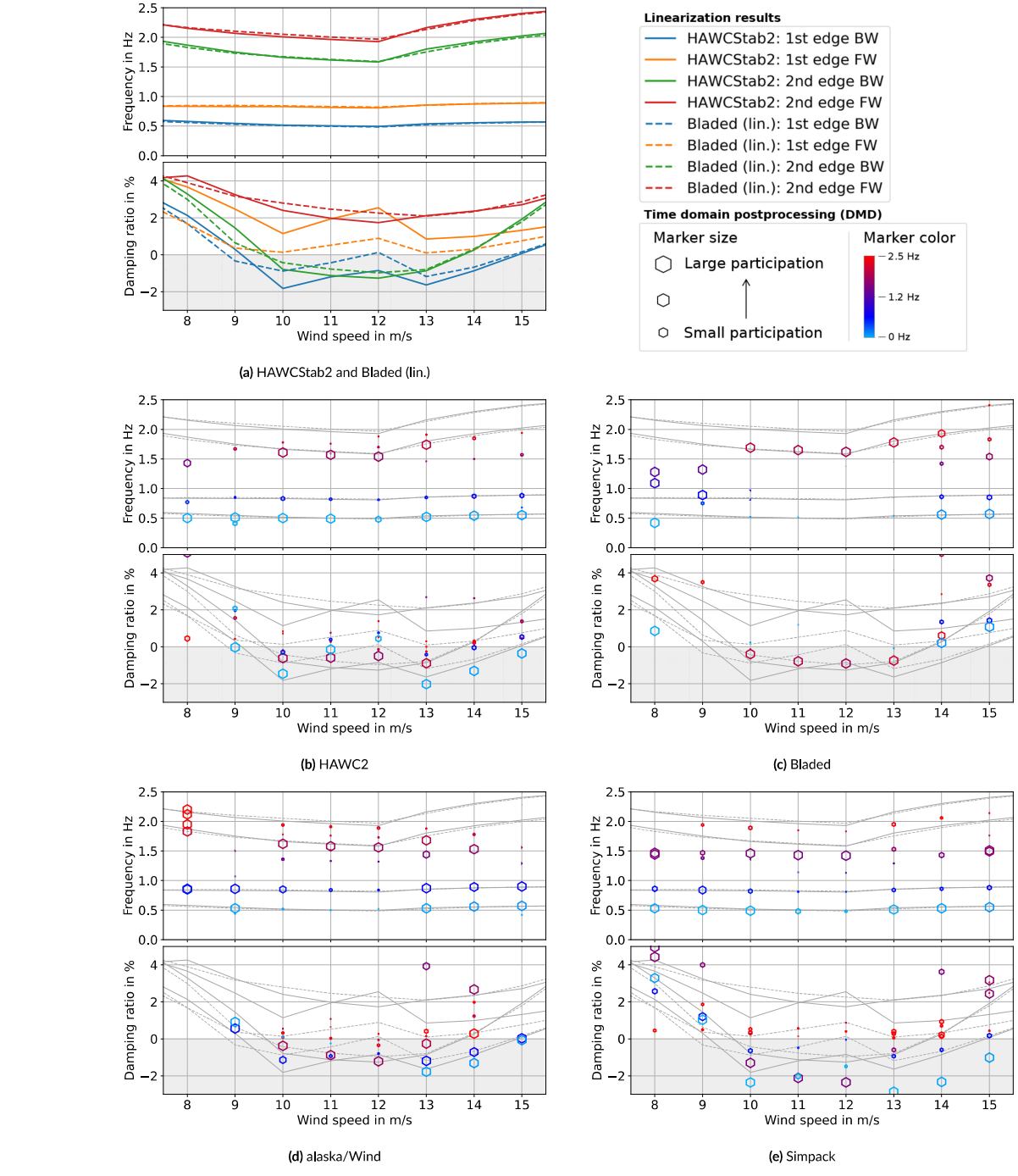

Figure 4. Linearizations (colored lines in (a), grey lines in (b-e)) and time domain simulations post-processed with DMD (markers in (b-e)).

https://doi.org/10.5194/wes-2023-80
Preprint. Discussion started: 8 August 2023

3 Uncertainty quantification case studies

Two case studies were performed on the influence of structural beam properties on the critical reference condition. Case study one is a basic study with a limited number of easily understandable uncertain parameters which serves as demonstration and verification of the overall process. Case study two is a step closer towards engineering practice and serves as a mock-up case study for the analysis of the influence of blade manufacturing defects on the aeroelastic stability.

The case studies are limited to the operating point at 12 m/s wind speed of the critical reference condition presented in Sect. 2. This can be interpreted as a single vertical slice of the Campbell diagrams in Fig. 4. The operating conditions (wind speed, rotor speed, pitch) are kept constant for all model variations during the uncertainty quantification. The damping ratio of the most critical mode was selected as the quantity of interest (QoI) for the uncertainty quantification, i.e., the influence of the uncertain parameters on the damping of this mode will be analyzed. The mode with the lowest damping at 12 m/s is for all tools the 2nd edgewise BW mode with a frequency of approximately 1.55 Hz and damping ratios varying between -2.35% and -0.5%.

3.1 Uncertainty Quantification (UQ) Framework

A non-intrusive, global, variance-based uncertainty quantification based on a PCE surrogate model will be used in this work. This methodology does not require a modification of the simulation codes and by means of the surrogate model, the required amount of simulations can be reduced significantly compared to a standard Monte-Carlo simulation. The uncertainty quantification covers the full domain spanned by the uncertain parameter distributions and captures the potential interaction between these parameters.

The Python implementation of the preprocessor, postprocessor, and interfaces to the tools is open-source available in the framework *wtuq* (Verdonck et al., 2023b, 2022). This framework uses the open-source packages *uncertainpy* and *chaospy* for the setup of the PCE model and uncertainty evaluation (Tennøe et al., 2018).

3.1.1 Surrogate model

Polynomial Chaos Expansion (PCE) with point collocation is used as surrogate model. The applied PCE models had a fourth order polynomial. The quasi-random Hammersley sampling scheme was used and the number of training data points for a given number of uncertain parameters were based on the best-practice findings by Hosder et al. (April 23–26, 2007). The accuracy of this setup was tested by decreasing and increasing the polynomial order and increasing the number of sampling points for some tools. This did not lead to significant improvements or deteriorations in the accuracy of the PCE model.

Verification of the PCE model is necessary to ascertain that the surrogate is a good representation of the true model. As initial verification measure, the surrogate model can be evaluated at the training data coordinates. However, this measure can be influenced by overfitting. Therefore, the leave-one-out test should be used as cross validation. This test is done by the computation of an individual leave-one-out surrogate model for each of the training data points. This surrogate model does not contain that specific training data point. A comparison of this leave-one-out surrogate model evaluated at the coordinates of the

https://doi.org/10.5194/wes-2023-80
Preprint. Discussion started: 8 August 2023

training data point and the true model evaluation at those coordinates is then done. In general, the computation of the surrogate model is not expensive, but as shown by Le Gratiet et al. (2017), an exact mathematical computation of the leave-one-out error without recomputation of the surrogate model for each of the training data points is also possible.

Alternatively, additional random control points, which are not entailed in the training dataset, could be used for verification. The leave-one-out error has the benefit over adding random control point computations, that no additional simulations are required. The downside is that the leave-one-out error might introduce additional errors, especially at the edges of the input parameter space, because it assembles new surrogate models, missing the data point where the leave-one-out error is computed.

Based on the training data and the leave-one-out surrogate model, two error estimation metrics are defined, which are

$$\text{Normalized root-mean-square deviation, NRMSD} = \frac{\sqrt{\frac{\sum\left(\widehat{X}-X^*\right)^2}{n}}}{\max\left(X^*\right)-\min\left(X^*\right)}, \tag{1}$$

$$\text{Mean absolute error, MAE} = \frac{\sum\left|\widehat{X}-X^*\right|}{n}. \tag{2}$$

Here, X^* is the set of training data samples of the quantity of interest, $\widehat{X}$ is the set of approximated quantities of interest of the leave-one-out surrogate model, and n is the number of samples.

3.1.2 Uncertainty Quantification

The uncertainty quantification is done on the PCE surrogate model. It is common to use the Sobol indices as global uncertainty quantification metrics. They are a measure for the contribution of each uncertain input parameter to the variance of the output quantity of interest. Two Sobol indices will be used in this paper. The first order Sobol index is given by

$$S_i = \frac{\mathbb{V}\left[\mathbb{E}\left[X|Q_i\right]\right]}{\mathbb{V}\left[X\right]}, \tag{3}$$

and represents the isolated contribution of an uncertain parameter to the total output variance. $\mathbb{V}\left[\mathbb{E}\left[X|Q_i\right]\right]$ is the variance of the expected value of the quantity of interest X, given only the uncertainty distribution of the uncertain parameter Q_i. $\mathbb{V}\left[X\right]$ is the total variance of the quantity of interest, including all uncertain parameters. The total Sobol index is given by

$$S_{Ti} = 1 - \frac{\mathbb{V}\left[\mathbb{E}\left[X|Q_{-i}\right]\right]}{\mathbb{V}\left[X\right]}, \tag{4}$$

and represents the contribution of an uncertain parameter to the total output variance, including interactions with other parameters. $\mathbb{V}\left[\mathbb{E}\left[X|Q_{-i}\right]\right]$ is the variance of the quantity of interest given the contributions of all uncertain parameters, except the contribution of parameter Q_i.

https://doi.org/10.5194/wes-2023-80
Preprint. Discussion started: 8 August 2023

The Sobol indices condense the uncertainty into single values. This is a clear metric for both the contribution of a parameter to the total variance in a model and the interaction between parameters, but does not give insight in the way an uncertain parameter influences the quantity of interest. This detailed view can be given at a negligible computational cost by analyzing the polynomials of the PCE model along the different uncertain dimensions.

3.2 Case study one: verification

This case study applies three straightforward uncertain parameters: flapwise, edgewise and torsional stiffness of the blades. These uncertain parameters are given identical uncertainty distributions. The radial discretization of the uncertainties is determined by a Non-Uniform Rational B-Spline (NURBS), similar to the methodology proposed by Kumar et al. (2020). In this case, the spline is fixed at the root and tip of the blade and a single control point in the center determines the shape of the NURBS curve. This methodology has been shown in Verdonck et al. (2022). The uncertain parameters are uniformly distributed and resulted in a maximum modification of the nominal stiffness values in the center of the blade of approximately $\pm 5\,\%$.

Note that to guarantee a correct modification of the parameters in the different tools, said modifications are done directly on the reference 6x6 mass and stiffness matrices (Hodges, 2006). Each variation has been verified by a comparison of the structural blade eigenvalues in the different tools for the individual parameter modifications. The same procedure was used for the parameter modifications of case study two.

3.2.1 PCE model verification

The simulation tools are sampled with the quasi-random Hammersley scheme to generate 72 training data points for the surrogate models. As described in Sect. 3.1.1, a leave-one-out surrogate model is set up for each training data point. This model verifies the accuracy of the surrogate model if the given training data point is excluded from the training data basis. Figure 5 shows the leave-one-out surrogate model evaluations with respect to the training data points. A perfectly accurate representation of the simulation model by the leave-one-out surrogate model would result in the points lying on the straight line (red line in Fig. 5). A satisfying agreement is found for all tools. The error metrics defined in Sect. 3.1.1 are visualized in the bottom right of Fig. 5. The mean absolute error (MAE) is a measure for the accuracy of the surrogate model to represent the training data. It has the same unit as the QoI, in this case the absolute damping ratio. The Normalized Root-Mean-Square Deviation (NRMSD) expresses its accuracy normalized by the bandwidth of damping values. The MAE figure shows that most surrogate models represent the training data with an error smaller than 0.01 % damping. The alaska/Wind surrogate model has the largest error. Nevertheless, the MAE is smaller than 0.04 % damping and the relative error is approximately 2.5 %, which is still very small and almost negligible.

https://doi.org/10.5194/wes-2023-80
Preprint. Discussion started: 8 August 2023

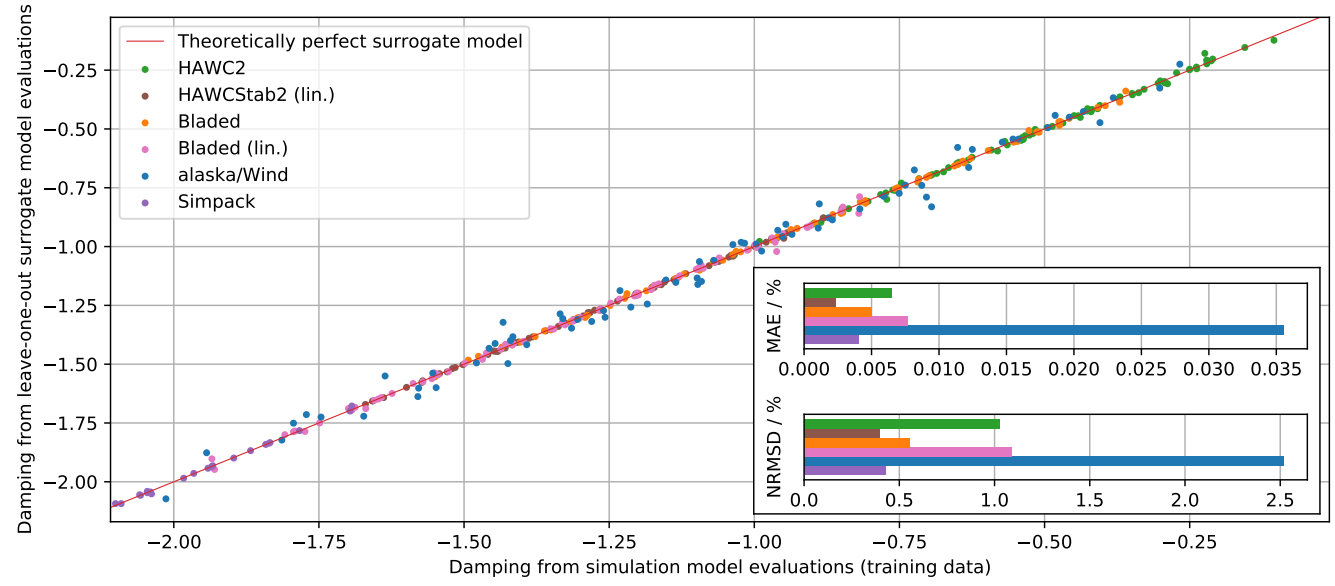

Figure 5. Case study 1: Comparison between leave-one-out surrogate model evaluations and training data samples

3.2.2 UQ results

The first order and total Sobol indices are shown in Fig. 6. The main finding is equivalent in all tools. The torsional stiffness, indicated by the green part of each of the pie charts, has the highest contribution towards the damping of the critical edgewise mode. The fact that the first order and total Sobol indices are nearly identical implies that the interaction among the uncertain parameters is not significant.

Two noticeable differences should be pointed out. Firstly, HAWC2 is the only model where the interaction between the uncertain parameters has a noteworthy contribution (4.12 %). Secondly, the sensitivity of the flapwise stiffness is significantly higher in Simpack and alaska/Wind compared to the other tools.

Figure 7 gives a more intuitive and simultaneously more detailed view on the first order effect of the isolated parameters. Each of the uncertain parameters is varied from its minimum to maximum value while keeping the other parameters constant at their mean value. This visualizes a single slice of the full uncertainty domain. The conclusions from the first order Sobol indices in Fig. 6 (top row) correlate well with the results in Fig. 7. The dominating sensitivity of the torsional stiffness is clear from the strong gradient (subplot on the right). In all tools the damping increases for an increasing torsional stiffness. The gradients of this sensitivity are overall similar, yet the curves are for some tools nonlinear, with locally highly different trends between the tools. The flapwise stiffness variation plot shows the sensitivity of the damping in Simpack and alaska/Wind. Here as well one can conclude that the overall gradient is similar, but the nonlinear trend is opposite. The sensitivity in Simpack seems to have a nonlinear convex shape, while the sensitivity in alaska/Wind has a nonlinear concave shape.

https://doi.org/10.5194/wes-2023-80
Preprint. Discussion started: 8 August 2023

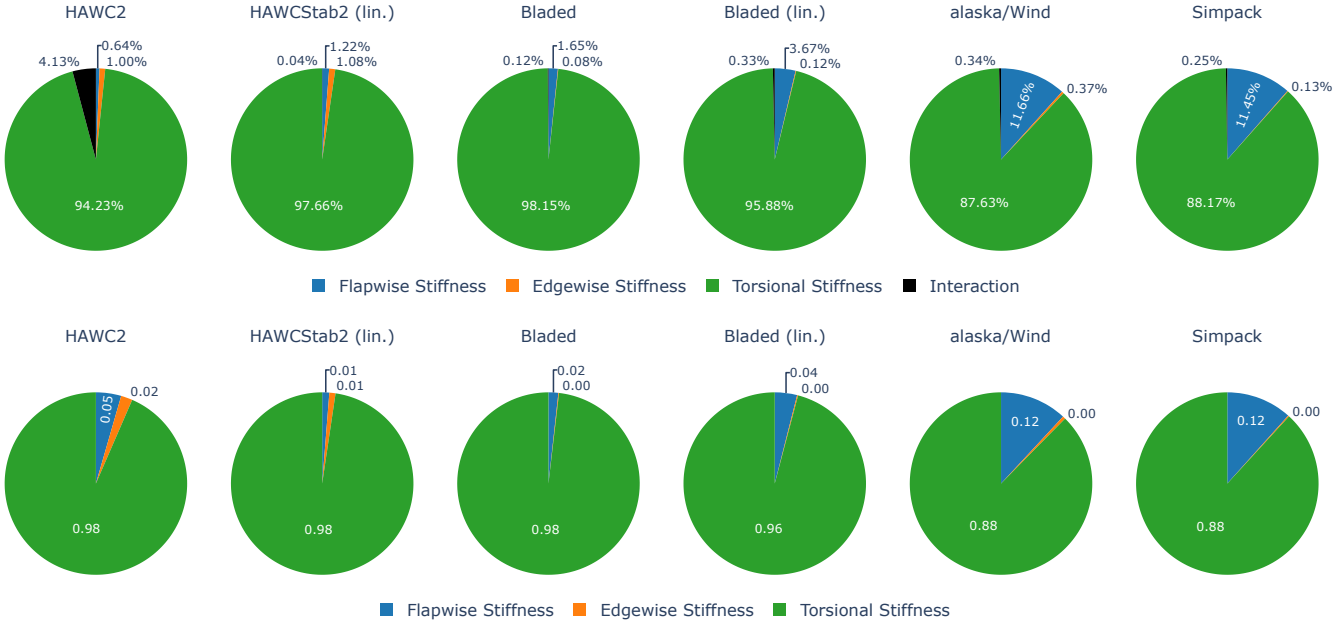

Figure 6. Case study 1: first order Sobol indices - isolated uncertainty contribution of the investigated parameters (**top row**), total Sobol indices - uncertainty contribution of the investigated parameters including interactions with other parameters (**bottom row**)

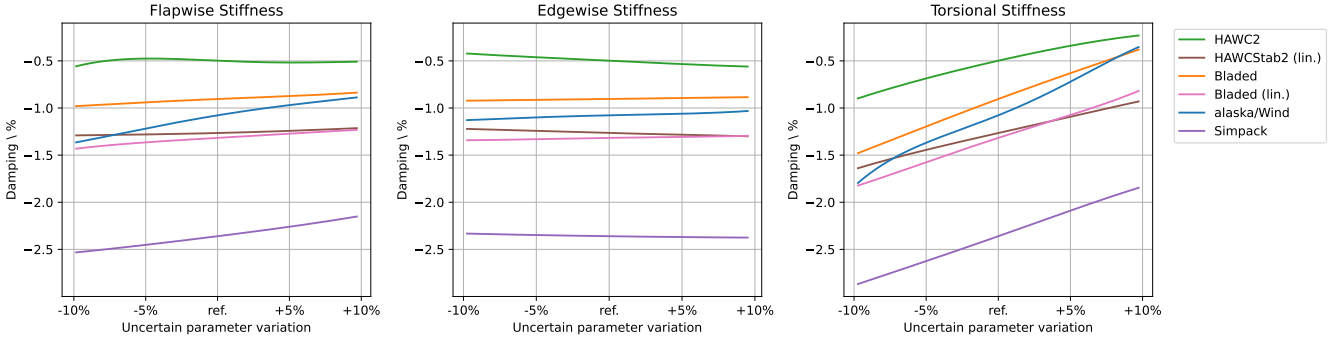

Figure 7. Case study 1: first order effects of an isolated parameter (other parameters at reference value)

3.3 Case study two: manufacturing defects

This case study was proposed to demonstrate a possible use case in the actual wind turbine development process and to show the comparability of the tools for more intricate uncertain parameters.

The edgewise stiffness, principal axis orientation, position of the center of gravity, and position of the shear centre along the chord are used as uncertain parameters. These beam properties are known to be sensitive towards manufacturing defects and assumed to have a significant impact on the stability. Noever-Castelos et al. (2021) investigated the influence of realistic

https://doi.org/10.5194/wes-2023-80
Preprint. Discussion started: 8 August 2023

manufacturing defects of the beam properties of the SmartBlades2 DemoBlade. The Gaussian distributions of these beam properties were scaled to the IWT reference blade, while retaining similar distributions along the blade. This approach is not intended to be exact or to result in a generally valid conclusion. Rather, it was attempted to use uncertainty distributions with physical meaning instead of using arbitrary, academic values.

3.3.1 PCE model verification

The leave-one-out verification and corresponding error metrics are shown in Fig. 8. The correlation is again satisfying in all tools. The largest dispersion and therefore highest error metrics can be seen for the Bladed linearization. The NRMSD is relatively high, with a maximum error of approximately 9 % for the Bladed (lin.) model. This is caused by the small bandwidth between maximum and minimum values, which is used to normalize the error. The small bandwidth implies that even a small error has a rather large normalized error. The MAE is in this case a better error indicator. For all tools the MAE remains below 0.015 % damping.

3.3.2 UQ results

The first order and total Sobol indices for case study 2 are shown in Fig. 9. Major differences in the uncertainty quantification appear. Overall, the chordwise COG and chordwise shear center position have the highest sensitivity. However, which of these two has the dominant uncertainty contribution, varies with the tools. HAWC2 and HAWCStab2 show a dominating uncertainty contribution by the chordwise shear center position. All other tools show a dominating contribution by the center of gravity position. The orientation of the principal axis has in all tools a negligible influence on the damping. The edgewise stiffness has a significant contribution to the overall variation in HAWC2, HAWCStab2, and Simpack, but a negligible contribution in Bladed, Bladed (lin.) and alaska/Wind. Similar to case study 1, the interaction between uncertain parameters has only a limited contribution to the overall damping variation.

Figure 10 visualizes the isolated influence of each parameter when all other parameters are kept at their nominal values. The principal axis orientation uncertain parameter is not shown, because it has a negligible uncertainty contribution in all tools. Especially interesting is the influence of the chordwise shear center position. In HAWC2 and HAWCStab2 the damping increases significantly if the shear center moves towards the trailing edge, which correlates with the higher Sobol indices seen in Fig. 9. The trends and/or gradients in the other tools are completely different. Note that the uncertain parameter variation in all tools has been verified by comparison of the structural blade eigenfrequencies. The differences which appear here are therefore due to the instability mechanism as a whole. This figure also exposes the limitations of the condensation of the parameter sensitivities to Sobol indices. Bladed, Bladed (lin.), and alaska/Wind have similar Sobol indices for the chordwise SC parameter, yet the dependency of the damping on this parameter appears to be highly different between these tools. The isolated effect of the chordwise COG position is more similar for all tools. All tools show a decrease in damping for a backward moving COG. In alaska/Wind, the gradient is significantly larger. Increasing the edge stiffness has a destabilizing effect in HAWCStab2, HAWC2, and Simpack, but a negligible sensitivity in Bladed, Bladed (lin.) and alaska/Wind.

https://doi.org/10.5194/wes-2023-80
Preprint. Discussion started: 8 August 2023

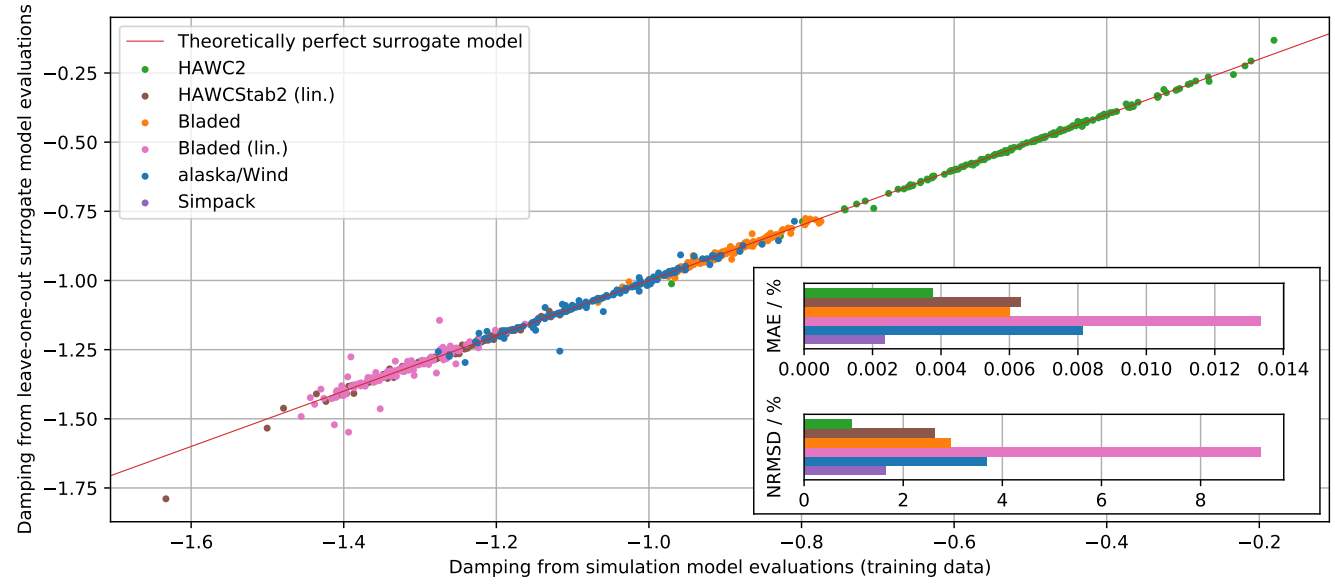

Figure 8. Case study 2: comparison between leave-one-out surrogate model evaluations and training data samples

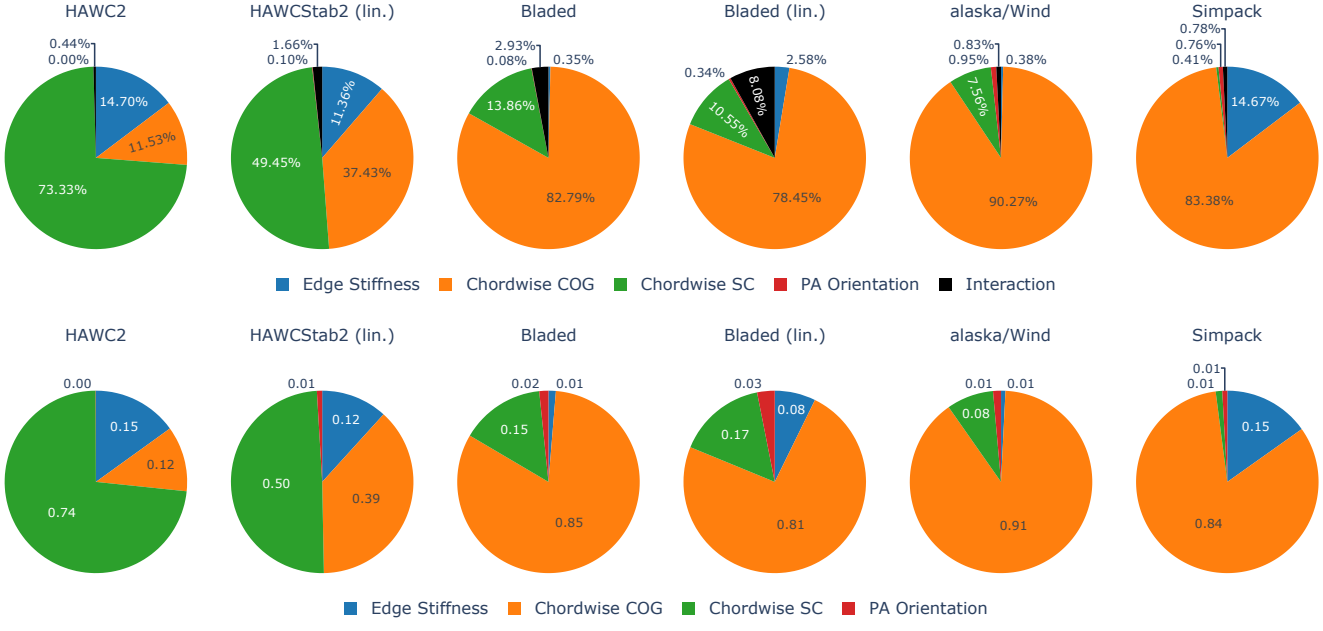

Figure 9. Case study 2: first order Sobol indices - isolated uncertainty contribution of the investigated parameters (**top row**), total Sobol indices - uncertainty contribution of the investigated parameters including interactions with other parameters (**bottom row**)

https://doi.org/10.5194/wes-2023-80
Preprint. Discussion started: 8 August 2023

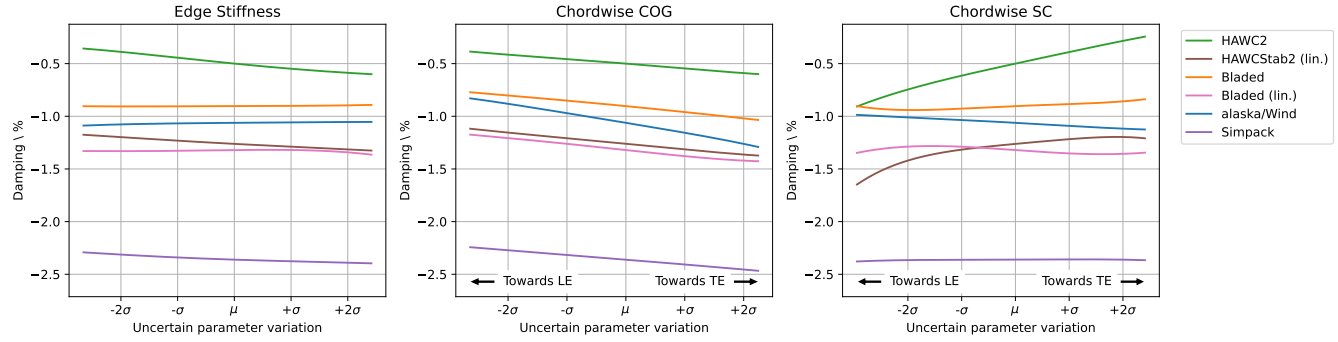

Figure 10. Case study 2: first order effects of isolated parameter (other parameters at reference value)

4 Conclusions

Models for multi-body simulations of wind turbines consist even in the described low-fidelity case of a huge number of parameters describing the degrees of freedom - especially for the blade. Evaluating and understanding the influence of each of these parameters on the aeroelastic stability of the model is complex. Sophisticated uncertainty quantification methods have to be used to assess the sensitivity in both a mathematically rigorous and computationally efficient manner.

In this work a code-to-code comparison between industry-relevant low-fidelity aeroelastic simulation tools (alaska/Wind, Bladed, HAWC2/HAWCStab2 and Simpack) has been done on the sensitivity of beam structural parameters on an edgewise whirling instability. The edgewise whirling instability was established on the IWT reference turbine by a reduction of the blade stiffness. To enable the comparison of time domain and linearization tool results, a dynamic mode decomposition (DMD) postprocessing methodology for non-linear time domain simulation has been introduced. This procedure was tuned for the identification of the unstable modes and should be developed further if it is to be applied on all operating conditions and all aeroelastic modes. The comparison of the reference condition showed an overall satisfying agreement between the tools. An accurate match of the frequency of the edgewise modes of the aeroelastic system in the selected operating states could be found in almost all tools. The modal damping showed similar trends over the operating points, but noticeable differences in the absolute values. A detailed study of the instability mechanism and the possible differences in the separate tools was out of the scope.

A PCE surrogate model was used in the uncertainty quantification to reduce the computational cost. The PCE models were successfully verified by means of leave-one-out tests, which proves that these models are well suited to represent the full uncertainty domain. Case study one showed equivalent sensitivities in all tools with a dominating influence of the torsional stiffness compared to flapwise and edgewise stiffness. Major differences between the tools appeared in case study two. The dominating uncertain parameter and the trend of the sensitivities were vastly different. In both case studies, the interaction between the uncertain parameters was limited, which would imply that the uncertainty quantification could have been done at an equal accuracy, but significantly lower computational cost. It is important to note that the results of both case studies depend on the presented simulation models, the instability mechanism itself and the selection and definition of the uncertain

https://doi.org/10.5194/wes-2023-80
Preprint. Discussion started: 8 August 2023

parameters and quantity of interest. The generalization of these results is difficult and should be made with caution. The case studies only covered a small number of uncertain parameters. In the future, it would be interesting to extend this to other, also non-structural, parameters. Furthermore, the input uncertainty distributions should be based on realistic deviations, e.g. by known uncertainties due to manufacturing imperfections or degradation over its lifetime.

Code and data availability. The code of the uncertainty quantification framework used for this study is available at https://github.com/DLR-AE/wtuq (Verdonck et al., 2023b). The data is available at https://doi.org/10.5281/zenodo.8134456 (Verdonck et al., 2023a).

Author contributions. HV was the main developer for the framework and the methodology in collaboration with OH. HV did the overall verification and analysis of the results in close collaboration with all other authors. HV and OH wrote the first version of the paper, internal review was done by CB and JR. SM was responsible for the simulation and analysis of the alaska/Wind results. JDP was responsible for the simulation and analysis of OpenFAST and co-responsible for the simulation and analysis of HAWC2 and HAWCStab2. OB was co-responsible for the simulation and analysis of HAWC2 and HAWCStab2 and made valuable contributions to the uncertainty quantification framework. JR generated the HAWC2 model and was the main source of information for the beam properties preprocessing. OH and CB were the principal investigators at DLR and LUH and supervised the contributions of their groups. All authors contributed to this research through discussions and advice in their respective fields of expertise.

Competing interests. The authors declare that they have no competing interests.

Acknowledgements. This work is a collaboration of three partners from research and industry in the frame of the German national research project *QuexUS*. This project was funded by the German Federal Ministry for Economic Affairs and Climate Action, grant no. 03EE3011A/B. Many thanks to the DTU HAWC2/HAWCStab2 development team for support and improvement during the active phase of simulations and to the DNV Bladed development team for their support and advice.

https://doi.org/10.5194/wes-2023-80
Preprint. Discussion started: 8 August 2023

eawe european academy of wind energy
Open Access WIND ENERGY SCIENCE DISCUSSIONS

References

Abbiati, G., Marelli, S., Tsokanas, N., Sudret, B., and Stojadinović, B.: A global sensitivity analysis framework for hybrid simulation, Mechanical Systems and Signal Processing, 146, 964–979, https://doi.org/10.1016/j.ymssp.2020.106997, 2021.

Bir, G.: Multi-Blade Coordinate Transformation and its Application to Wind Turbine Analysis, in: 46th AIAA Aerospace Sciences Meeting and Exhibit, AIAA, Reno, Nevada, https://doi.org/10.2514/6.2008-1300, 2008.

Blasques, J. P., Bitsche, R. D., Fedorov, V., and Lazarov, B. S.: Accuracy of an efficient framework for structural analysis of wind turbine blades, Wind Energy, 19, 1603–1621, https://doi.org/10.1002/we.1939, 2016.

Bortolotti, P., Canet, H., Bottasso, C. L., and Loganathan, J.: Performance of non-intrusive uncertainty quantification in the aeroservoelastic simulation of wind turbines, Wind Energy Science, 4, 397–406, https://doi.org/10.5194/wes-4-397-2019, 2019.

Caboni, M., Carrion, M., Rodriguez, C., Schepers, G., Boorsma, K., and Sanderse, B.: Assessment of sensitivity and accuracy of BEM-based aeroelastic models on wind turbine load predictions, in: J. Phys.: Conf. Ser., vol. 1618, TORQUE, Delft, The Netherlands, https://doi.org/10.1088/1742-6596/1618/4/042015, 2020.

Eldred, M. and Burkardt, J.: Comparison of Non-Intrusive Polynomial Chaos and Stochastic Collocation Methods for Uncertainty Quantification, in: 47th AIAA Aerospace Sciences Meeting including The New Horizons Forum and Aerospace Exposition, Sandia National Laboratories, https://doi.org/10.2514/6.2009-976, iSBN 978-1-60086-973-0, 2009.

Gonzaga, P., Toft, H., Worden, K., Dervilis, N., Bernhammer, L., Stevanovic, N., and Gonzales, A.: Impact of blade structural and aerodynamic uncertainties on wind turbine loads, Wind Energy, https://doi.org/10.1002/we.2715, 2022.

Hach, O., Verdonck, H., Polman, J. D., Balzani, C., Müller, S., Rieke, J., and Hennings, H.: Wind turbine stability: Comparison of state-of-the-art aeroelastic simulation tools, in: J. Phys.: Conf. Ser, vol. 1618, TORQUE, IOP Publishing, https://doi.org/10.1088/1742-6596/1618/5/052048, 2020.

Hodges, D. H.: Nonlinear Composite Beam Theory, AIAA, https://doi.org/10.2514/4.866821, 2006.

Hosder, S., Walters, R., and Balch, M.: Efficient Sampling for Non-Intrusive Polynomial Chaos Applications with Multiple Uncertain Input Variables, in: 48th AIAA/ASME/ASCE/AHS/ASC Structures, Structural Dynamics, and Materials Conference, AIAA, Honolulu, Hawaii, April 23–26, 2007.

Hübler, C., Gebhardt, C. G., and Rolfes, R.: Hierarchical four-step global sensitivity analysis of offshore wind turbines based on aeroelastic time domain simulations, Renewable Energy, 111, 878–891, https://doi.org/10.1016/j.renene.2017.05.013, 2017.

Hübler, C., Gebhardt, C. G., and Rolfes, R.: Assessment of Sensitivity Analysis Methods of Different Complexity for Offshore Wind Turbines, in: 29th European Safety and Reliability Conference, ESREL, Hannover, Germany, https://doi.org/10.3850/978-981-11-2724-3_0140-cd, 2019.

IEC: IEC 61400-1 Edition 3 - Wind Turbines - Part 1: Design requirements, Tech. rep., International Electrotechnical Commission, Geneva, 2005.

Iooss, B. and Lemaître, P.: A Review on Global Sensitivity Analysis Methods, pp. 101–122, Springer US, Boston, MA, 2015.

Kallesøe, B. S. and Kragh, K. A.: Field Validation of the Stability Limit of a Multi MW Turbine, in: J. Phys.: Conf. Ser, vol. 753, TORQUE, Munich, Germany, https://doi.org/10.1088/1742-6596/753/4/042005, 2016.

Kumar, P., Sanderse, B., Boorsma, K., and Caboni, M.: Global sensitivity analysis of model uncertainty in aeroelastic wind turbine models, in: J. Phys.: Conf. Ser, vol. 1618, TORQUE, Delft, The Netherlands, https://doi.org/10.1088/1742-6596/1618/4/042034, 2020.

https://doi.org/10.5194/wes-2023-80
Preprint. Discussion started: 8 August 2023

Le Clainche, S. and Vega, J.: Higher Order Dynamic Mode Decomposition, SIAM Journal on Applied Dynamical Systems, 16, 882–925, https://doi.org/10.1137/15M1054924, 2017.

Le Gratiet, L., Marelli, S., and B, S.: Metamodel-Based Sensitivity Analysis: Polynomial Chaos Expansions and Gaussian Processes, pp. 1289–1325, Springer, https://doi.org/10.1007/978-3-319-12385-1_38, 2017.

Li, S. and Caracoglia, L.: Surrogate Model Monte Carlo simulation for stochastic flutter analysis of wind turbine blades, Journal of Wind Engineering and Industrial Aerodynamics, 188, 43–60, https://doi.org/10.1016/j.jweia.2019.02.004, 2019.

Lobitz, D. W.: Parameter Sensitivities Affecting the Flutter Speed of a MW-Sized Blade, Journal of Solar Energy Engineering, 127, 538–543, https://doi.org/10.1115/1.2037091, 2005.

Noever-Castelos, P., Ardizzone, L., and Balzani, C.: Model updating of wind turbine blade cross sections with invertible neural networks, Wind Energy, https://doi.org/10.1002/we.2687, 2021.

NREL: Reference to known issues in BeamDyn, https://github.com/OpenFAST/openfast/issues/366, accessed: 2022-02-03, 2019.

Pirrung, G. R., Madsen, H. A., and Kim, T.: The influence of trailed vorticity on flutter speed estimations, in: J. Phys.: Conf. Ser, vol. 524, TORQUE, IOP Publishing, https://doi.org/10.1088/1742-6596/524/1/012048, 2014.

Popko, W. et al.: IWES Wind Turbine IWT-7.5-164. Rev 4, Tech. rep., Fraunhofer IWES, Bremerhaven, Germany, https://gitlab.cc-asp.fraunhofer.de/iwt/iwt-7.5-164, GPL v3, 2018.

Pourazarm, P., Caracoglia, L., Lackner, M., and Modarres-Sadeghi, Y.: Stochastic analysis of flow-induced dynamic instabilities of wind turbine blades, Journal of Wind Engineering and Industrial Aerodynamics, 137, 37–45, https://doi.org/10.1016/j.jweia.2014.11.013, 2015a.

Pourazarm, P., Modarres-Sadeghi, Y., and Lackner, M.: A parametric study of coupled-mode flutter for MW-size wind turbine blades: Coupled-mode flutter of MW-size wind turbine blades, Wind Energy, 19, 497–514, https://doi.org/10.1002/we.1847, 2015b.

Resor, B. and Paquette, J.: Uncertainties in Prediction of Wind Turbine Blade Flutter, in: 52nd AIAA/ASME/ASCE/AHS/ASC Structures, Structural Dynamics and Materials Conference, American Institute of Aeronautics and Astronautics, Denver, Colorado, https://doi.org/10.2514/6.2011-1947, 2011.

Riziotis, V. and Voutsinas, S.: Advanced aeroelastic modeling of complete wind turbine configurations in view of assessing stability characteristics, in: Proceedings of the EWEC '06, EWEA, Athens, Greece, 2006.

Roberson, A. N., Shaler, K., Sethuraman, L., and Jonkman, J.: Sensitivity analysis of the effect of wind characteristics and turbine properties on wind turbine loads, Wind Energy Science, 4, 479–513, https://doi.org/10.5194/wes-4-479-2019, 2019.

Sankararaman, S.: Uncertainty quantification and integration in engineering systems, Ph.D. thesis, Vanderbilt University, 2012.

Sudret, B.: Global sensitivity analysis using polynomial chaos expansion, Reliability Engineering and System Safety, 93, 964–979, https://doi.org/10.1016/j.ress.2007.04.002, 2008.

Tennøe, S., Halnes, G., and Einevoll, G. T.: Uncertainpy: A Python Toolbox for Uncertainty Quantification and Sensitivity Analysis in Computational Neuroscience, Frontiers in Neuroinformatics, 12, https://doi.org/10.3389/fninf.2018.00049, 2018.

van den Bos, L. M. M. and Sanderse, B.: Uncertainty quantification for wind energy applications - Literature review, Tech. Rep. SC-1701, Centrum Wiskunde & Informatica, 2017.

Veers, P. et al.: Grand challenges in the science of wind energy, Science, 366, 2019.

Verdonck, H., Hach, O., Braun, O., Polman, J. D., Balzani, C., Müller, S., and Rieke, J.: Code-to-code comparison of realistic wind turbine instability phenomena, Presentation, https://doi.org/10.5281/zenodo.5874658, Presented at the Wind Energy Science Conference (WESC), https://doi.org/10.5281/zenodo.5874658, 2021.

https://doi.org/10.5194/wes-2023-80
Preprint. Discussion started: 8 August 2023

Verdonck, H., Hach, O., Polman, J. D., Braun, O., Balzani, C., Müller, S., and Rieke, J.: An open-source framework for the uncertainty quantification of aeroelastic wind turbine simulation tools, in: J. Phys.: Conf. Ser, vol. 2265, TORQUE, Delft, The Netherlands, https://doi.org/10.1088/1742-6596/2265/4/042039, 2022.

Verdonck, H., Hach, O., Balzani, C., Polman, J. P., Braun, O., Rieke, J., and S, M.: QuexUS Data Package, Open-access dataset on Zenodo, https://doi.org/10.5281/zenodo.8134456, 2023a.

Verdonck, H., Hach, O., Balzani, C., Polman, J. P., Braun, O., Rieke, J., and S, M.: wtuq v1.1, Wind Turbine Uncertainty Quantification, Open-source software on Zenodo, https://doi.org/10.5281/zenodo.8133824, 2023b.

Volk, D., Kallesøe, B., Johnson, S., Pirrung, G., Riva, R., and Barnaud, F.: Large wind turbine edge instability field validation, in: J. Phys.: Conf. Ser, vol. 1618, TORQUE, Delft, The Netherlands, https://doi.org/10.1088/1742-6596/1618/5/052014, 2020.

Wanke, G., Bergami, L., and Verelst, D. R.: Differences in damping of edgewise whirl modes operating an upwind turbine in a downwind configuration, Wind Energy Science, 5, 929–944, https://doi.org/10.5194/wes-5-929-2020, 2020.

Ziegler, L. and Muskulus, M.: Fatigue reassessment for lifetime extension of offshore wind monopile substructures, in: J. Phys.: Conf. Ser., vol. 753, TORQUE, Munich, Germany, https://doi.org/10.1088/1742-6596/753/9/092010, 2016.